Properties of Dislocations in HgCdTe Crystals

P. Renault, J-F. Barbot, P. Girault, A. Declemy, G. Rivaud, C. Blanchard

HAL Id: jpa-00249388

https://hal.science/jpa-00249388

Submitted on 4 Feb 2008

Properties of Dislocations in HgCdTe Crystals

P.O. Renault([1]), J.F. Barbot([1]), P. Girault([2]), A. Declemy([1]), G. Rivaud([1]) and
C. Blanchard([1])

([1]) Laboratoire de Métallurgie Physique, URA 131 CNRS, Université de Poitiers, 40 av. du
Recteur Pineau, 86022 Poitiers cedex, France
([2]) LEMMA Université de La Rochelle, Pôle Science et Technologie, av. Marillac, 17042 La
Rochelle cedex 1, France

Abstract. — Dislocations in $Hg_{1-x}Cd_xTe$ ($x \approx 0.2$) single crystals have been introduced either
by plastic deformation or by Al-implantation at high dose. Structural analysis of implanted
samples, using Huang's method shows that dislocation loops are mainly of interstitial type with
a radius of about 2.6 nm. Electrical properties of uniaxially deformed samples, using Hall effect,
indicate the presence of both acceptor-like type dislocations along with donor-type point defects.

1. Introduction

The solid solutions $Hg_{1-x}Cd_xTe$ have important technological applications for infrared devices.
The device performances are known to be affected by the presence of extended defects, such as
dislocations. All results concerning their electrical properties can be explained assuming that
dislocations produce electronic trap states in the band gap acting as Shockley-Read centres.
Recent articles have been published on the effects of dislocations on HgCdTe devices [1–3]. For
example, Shin *et al.* [1] have shown that the minority-carrier lifetime is inversely proportional
to the dislocation density for densities higher than 5×10^5 cm^{-2}. Such dislocation densities are
currently observed in HgCdTe, especially in epitaxially grown materials. A review of dislocation
density depending on the growth method is given in reference [4]. Moreover, HgCdTe being very
soft and brittle, dislocations can be easily introduced during the process as well as by handling.
At this time, little is known, in comparison with elemental semiconductors, about general
features of dislocation dynamics in these materials. We have thus performed experiments on
HgCdTe single crystals where dislocations have been introduced either by ion implantation
at high fluence or by plastic deformation. Ion implantation which is used in manufactering
junctions for infrared $Hg_{1-x}Cd_xTe$ ($x \approx 0.2-0.3$) detectors and for optoelectronic $Hg_{1-x}Cd_xTe$
($x \approx 0.7$) components ($\lambda = 1.3$ μm), has been found to produce dislocations, the structure of
which is presented in Section 2. The electrical properties of dislocations, discussed in Section
3, have been studied on plastically deformed samples. Concluding remarks are finally given in
Section 4.

All our experiments have been performed on $< 111 >$ oriented $Hg_{1-x}Cd_xTe$ ($x \approx 0.2$) crystals grown by the Travelling Heater Method (THM) at SAT (Poitiers). Measurements of the intensity distribution around the reciprocal-lattice points have been made using a focusing quartz monochromator and copper $K\alpha_1$ radiation delivered by a 5-kW rotating anode X-ray tube. The Van der Pauw pattern was used to carry out the electrical measurements. The samples which have been deformed at room temperature by uniaxial stress along [123] axis ($\dot{\gamma} \approx 6 \times 10^{-6}$ s^{-1}) were placed on the cold finger of a cryogenerator (Leybold Heraus, RW2) whose temperature could be set within 1 K in the range 15-300 K.

2. Dislocation Structure on Implanted HgCdTe Crystals

In II-VI semiconductors, dislocation loops can be induced, at room temperature, by ion implantation or electron irradiation. The nature of these loops depends on the crystal structure, wurtzite or zincblende. In CdTe, all those identified were of interstitial type lying in the $\{111\}$ plane, the majority being Frank loops with a Burgers vector $b = a/3 < 111 >$ normal to the plane [5]. These results are different from those observed in III-V compounds of zincblende structure, for which dislocation loops with Burgers vector $a/2 < 110 >$ are observed. The fact that faulted loops have never been observed in III-V compounds, is explained by the larger stacking fault energy compared to that in II-VI compounds. This is correlated to the ionicity of crystals [6] which varies from 0.6 to 0.7 for II-VI compounds (ZnS, ZnSe, CdS and CdTe) and is approximately 0.3 for III-V compounds like GaSb, GaAs, InSb and GaP.

For the solid solution HgCdTe, many authors [7–10] have also shown the presence of dislocation loops under particular conditions of implantation. However, their small size has made their characterization difficult and contradictory results have been obtained. So, in order to distinguish unambiguously between the nature of the loops, intensity measurements of X-ray diffuse scattering near Bragg reflection has been carried out. Figure 1 shows a typical intensity Curve for a [440] reflection in the direction [110], measured at 300 K on $Hg_{1-x}Cd_xTe$ ($x = 0.2$) implanted at a dose of 3×10^{14} Al cm^{-2} The ion energy was fixed at 320 keV ($R_P \approx 380$ nm). q measures the deviation from the Bragg reflection and h is a reciprocal lattice vector. The defect-induced diffuse scattering intensity $I^{\text{diff}}(q)$ was obtained by subtracting the scattering background $I^{\text{ref}}(q)$ (measured on the sample before implantation) from the total scattering $I^{\text{impl}}(q)$ measured after ion implantation $I^{\text{diff}}(q) = I^{\text{impl}}(q) - I^{\text{ref}}(q)$. Close to the reciprocal lattice points, an asymmetry of the scattering is clearly observed, $I^{\text{diff}}(+q) > I^{\text{diff}}(-q)$. For defects, as for dislocation loops, the sign of the asymmetric scattering, $I^{\text{diff}}_{\text{asym}}(q) = \dfrac{I^{\text{diff}}(+q) - I^{\text{diff}}(-q)}{2}$ determines the sign of the displacement field around the defect. Since the diffuse scattering is more pronounced towards the positive values of q/h, it can be clearly concluded that the majority of dislocation loops induced by the ion implantation are of interstitial type. This result confirms previously reported TEM (Transmission Electron Microscopy) observations [7] for boron implantation. We must note that, for a dose of 5×10^{15} Al cm^{-2}, dislocation lines with a Burger vector $a/2 < 110 >$ have also been observed by TEM.

Informations can also be deduced from the symmetric part of the diffuse intensity $I^{\text{diff}}_{\text{sym}}(q) = \dfrac{I^{\text{diff}}(+q) + I^{\text{diff}}(-q)}{2}$ For low point defect concentrations ($c \ll 1$), close to the Bragg peaks, the scattering (Huang scattering) mainly yields information about the long-range part of the displacement field of the defect. For defect clusters, the Huang scattering ($I_{\text{H}} \propto 1/q^2$) is restricted to a region of quite small values of q ($q \ll 1/R_{\text{cl}}$ where R_{cl} is the mean radius of the clusters) and gives information about the symmetry of the long-range displacement field of the clusters. For larger q ($q > 1/R_{\text{cl}}$), the contribution of the highly distorted surrounding of
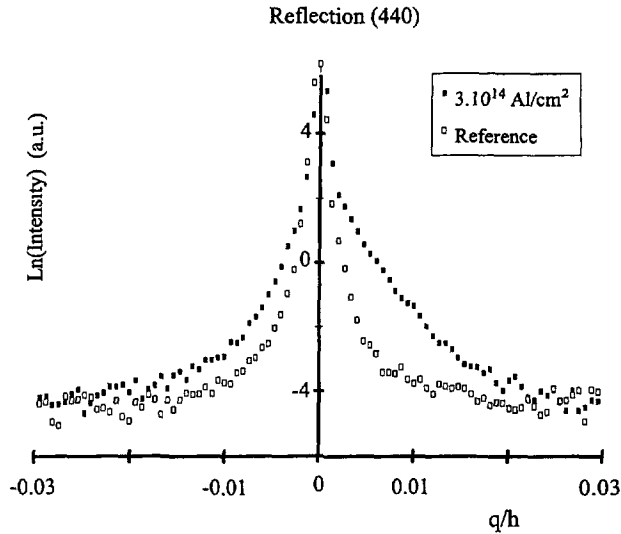
Fig. 1. — Intensity near the [440] reflection in the [110] direction. Measurements were performed at T=300 K, in $Hg_{0.8}Cd_{0.2}Te$ implanted ($E = 320$ keV, $\phi = 3 \times 10^{14}$ Al cm^{-2}).

the clusters dominates the scattering (Stokes-Wilson scattering $I_{S.W.}$). So, far from the Bragg reflections the intensity falls off as $1/q^4$ ($I_{S.W.} \propto 1/q^4$). The q-value where the change of slope is observed gives a critical radius $R_{crit} = 1/q_c$, the R_{crit} is often used for an estimate of the cluster radius R_{cl} [11–13]. Figure 2 shows a double-logarithmic plot of the defect scattering as obtained directly after 3×10^{14} Al/cm^2 ion implantation at 300 K. For very small values of q/h, we see the $1/q^2$ behavior of the Huang scattering. At larger distances from the Bragg reflection, the intensity drops as $1/q^4$ (Stokes-Wilson approximation). The transition determines a mean cluster radius of implantation defects $R_{cl} = 2.6 \pm 0.4$ nm. This method gives a precise value of the mean loop radius in comparison to previous works obtained using TEM for which dislocation loops were found only to be lower than 10 nm [10].

3. Electronic Properties of Deformed HgCdTe Crystals

Most of the measurements have been performed on plastically deformed n-type $Hg_{0.8}Cd_{0.2}Te$ samples ($E_G = 0.16$ eV at 20 K). HgCdTe deforms by slip on $\{111\} < 1\bar{1}0 >$ as for elemental and III-V semiconductors for which the dislocation motion takes place along the so-called Peierls-Nabarro mechanism. Moreover, dislocations with $b = a/2 < 110 >$ are dissociated into two Shockley partials ($b_p = a/6 < 112 >$) with a stacking fault energy $\gamma \approx 12 \pm 2$ mJ/m^2 corresponding to $\gamma/b_p = 45 \pm 7$ MPa [14]. Figures 3a and 3b respectively give the variations of the Hall coefficient R_H and the Hall mobility μ_H versus deformation. The data show that the defects introduced by plastic deformation lead to a systematic increase of the resistivity with deformation. The Hall mobility μ_H decreases with increasing deformation. In the temperature range 18-50 K, μ_H falls from 3×10^5 cm^2 V^{-1} s^{-1} before deformation to 300 cm^2 V^{-1} s^{-1} after 12% deformation, Figure 3b. On the other hand, the variations of the Hall coefficient R_H are different according to the applied deformation (Fig. 3a). Indeed, at
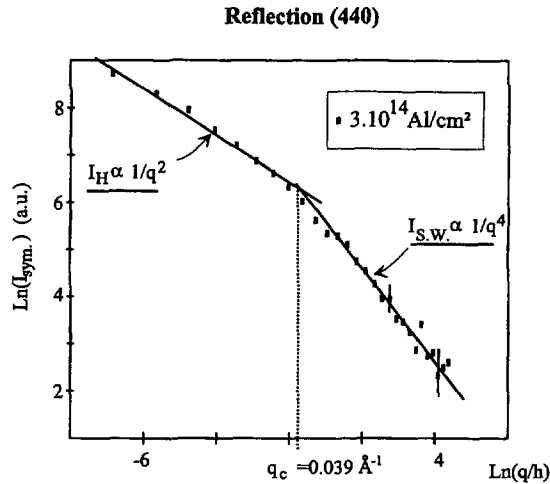
Reflection (440)

Fig. 2. — Symmetrical part of the scattering intensity measured after ion implantation $(3 \times 10^{14}$ Al cm$^{-2})$, the (440) reflection is in q direction [110].

a fixed low temperature (20 K) we observe a slight increase of $|R_H|$ for small deformations $(\delta l/l \leq 1\%)$ and then a continuous decrease of $|R_H|$ with increasing deformation. Such an increase in electron concentration for medium deformed Hg$_{0.8}$Cd$_{0.2}$Te $(\delta l/l = 2\%)$ has already been reported [15]. Applying for small deformations $(\delta l/l \leq 2\%)$ a model previously developed by Ferré [16] on GaAs, we have shown that dislocations introduce an acceptor like deep level located between E_v and $E_v + 40$ meV in n-type Hg$_{0.8}$Cd$_{0.2}$Te [17]. The observed decrease in $|R_H|$ with increasing deformation is interpreted as being the consequence of a large point defect density introduced by deformation. For small deformations the acceptor character of dislocations prevails whereas, with increasing deformation, the induced donor point defects have a concentration which exceeds dislocation trapping.

p-type HgCdTe has been less studied than n-type, nevertheless we observe in p-Hg$_{0.8}$Cd$_{0.2}$Te deformed samples an increase of the resistivity and only a decrease of $|R_H|$ with the deformation whatever the applied magnetic field B may be in the range 1- 5 kG. So, it seems that the defects introduced by the deformation have an acceptor character. However, in contrast to what is observed for n-type samples the variations of the Hall coefficient between deformed and non deformed samples are weak; in this way results concerning p-type deformed Hg$_{0.8}$Cd$_{0.2}$Te are incomplete. As for the heavy hole mobility μ_{hh}, it falls from about 200 cm^2 V^{-1} s^{-1} before deformation to 70 cm^2 V^{-1} s^{-1} after 4% deformation (Fig. 4). In Cd-rich p-CdHgTe we have clearly demonstrated using Electron Beam Induced Current (EBIC) that a local deformation (microhardness) converts from p-type to n-type [18]. This is consistent with the observations obtained on deformed Hg-rich n-HgCdTe.

The results obtained in deformed CdTe [19] using Deep Level Transient Spectroscopy (DLTS) have shown that the level associated with deformation-induced dislocations should rather be attributed to the point defect atmosphere surrounding the dislocation than to dislocation core states themselves. At this time, although only speculations can be made for HgCdTe crystals, it seems as for CdTe that the electrical properties of dislocations are mainly determined by their
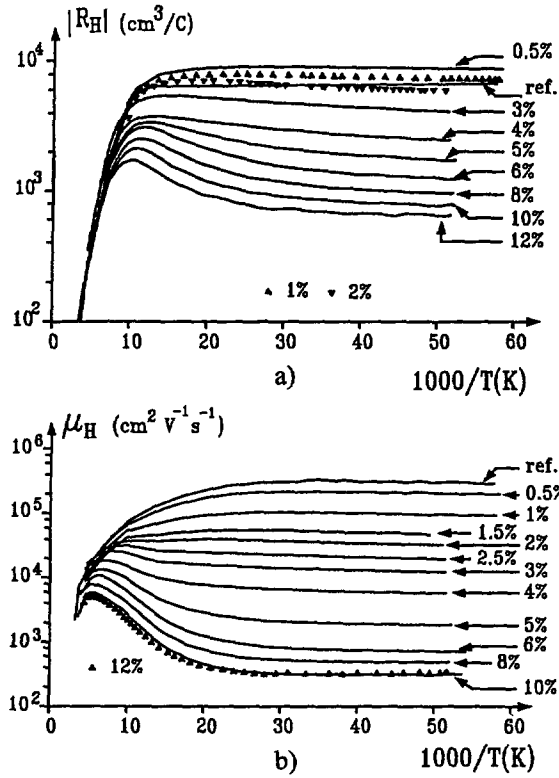
Fig. 3. — a) variations of the Hall mobility. b) Hall coefficient measurements on deformed n-$Hg_{0.8}Cd_{0.2}Te$ ($T = 300$ K, [123] axis) as a function of temperature for different strain values.
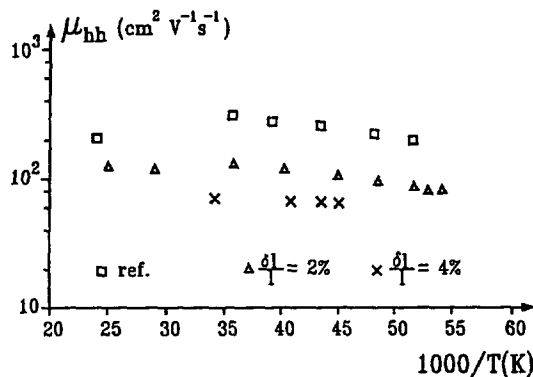

Fig. 4. — Variations of the heavy hole mobility on deformed p-$Hg_{0.8}Cd_{0.2}Te$ ($T = 300$ K, [123] axis) versus temperature for two strain values (2% and 4%). Each value of the mobility (symbols) has been deduced from the Hall coefficient variations with the applied magnetic field B (1, 3 and 5 kG) and from the value of the resistivity.

extrinsic effects, such as a change or a redistribution of point defects, rather than by the intrinsic ones due to their dangling bonds. Recently we have shown [20] that the dissociation of an acceptor-donor complex is possible in space-charge regions of HgCdTe crystals. Applying this dissociation to the model of interaction of such complex with moving charged dislocations [21] we can reasonably explain the large concentration of donor defects induced in n-type material by the deformation.

4. Concluding Remarks

Because of the high mobility of dislocations in HgCdTe crystals, even at low temperature, data regarding their motion are rather scarce. That makes their formation and multiplication during the growth process or their slip when the device is in operation easy. There seems to be similarities with mechanisms operating in III-V semiconductors, except for the fact that the temperature ranges are different. In this paper, using the Huang's method we have confirmed that dislocations loops in implanted HgCdTe crystals are majoritary interstitial in nature. Moreover, the size of loops has been evaluated to be about 2.6 nm for 320 keV implants of 5×10^{14} Al cm^{-2} Although the analysis of the electrical activity of dislocation is complicated, their contributions to the degradation on electrical properties of the materials clearly appear. Measurements on low deformed material have shown that clean dislocations must have an acceptor, character without taking into account the unavoidable decoration by impurity atoms. The surronding point defect cloud which prevails for large deformations has a donor like character.

References

[1] Shin S.H., Arias J.M., Zandian M., Pasko J.G. and DeWames R.E., Effect of the dislocation density on minority-carrier lifetime in molecular beam epitaxial HgCdTe, *Appl. Phys. Lett.* **59** (1991) 2718-2720.

[2] Johnson S.M., Rhiger D.R., Rosbeck J.P., Peterson J.M., Taylor S.M. and Boyd M.E., Effect of dislocations on the electrical and optical properties of long-wavelength infrared HgCdTe photo-voltaic detectors, *J. Vac. Sci. Technol.* **10** (1992) 1499-1506.

[3] List R.L., Formation and electrical effects of process induced dislocations in HgCdTe, *J. Vac. Sci. Technol.* **10** (1992) 1651-1657.

[4] Tregilgas J.H., Dislocations density of HgCdTe, Properties of Narrow Gap Cadmium based Compounds (emis datareviews series n°10, 1994) pp. 181-184.

[5] Gué A.M. and Mazel A., Etude expérimentale de la dynamique de croissance de défauts étendus, sous irradiation électronique à haute énergie dans le tellurure de cadmium, *J. Phys. France* **49** (1988) 53-61.

[6] Takeuchi S., Suzuki K., Maeda K. and Iwanaga H., Stacking-fault energy of II-VI compounds, *Phil. Mag.* **50** (1984) 171-178.

[7] Schaake H.F., Ion implantation damage in $Hg_{0.8}Cd_{0.2}Te$, *J. Vac. Sci. Technol.* **4** (1986) 2174-2176.

[8] Bubulac L.O., Tennant W.E., Riedel R.A. and Magee T.J., Behavior of implantation-induced defects in HgCdTe, *J. Vac. Sci. Technol.* **21** (1982) 251-254.

[9] Destéfanis C.L., Electrical doping of HgCdTe by ion implantation and heat treatment, *Nucl. Inst. and Meth.* **209/210** (1983) 567-580.

[10] Blanchard C., Barbot J.F., Cahoreau M., Desoyer J.C., LeScoul D. and Dessus J.L., Study of Al implantation in $Hg_{0.3}Cd_{0.7}Te$, *Nucl. Inst. and Meth. B* **47** (1990) 15-21.

[11] Dederichs P.H., The theory of diffuse X ray scattering and its application to the study of point defects and their clusters, *J. Phys. F.: Metals Phys.* **3** (1973) 471-496.

[12] Trinkaus H., On the Investigation of Small Dislocation Loops in Cubic Crystals by Diffuse X-Ray Scattering, *Phys. Stat. Sol. (b)* **54** (1972) 209-218.

[13] Von Guérard B. and Peisl J., Diffuse X-Ray scattering from copper after neutron irradiation at 4.6 K, in Fundamental aspects of radiation damage in metals, Proceedings of an International Conference held at Gatlinburg Tennessee, Vol. I (U.S.A., 1975) pp. 287-294.

[14] Barbot J.F., Hardness, yield stress and photoplastic effect in HgCdTe, Properties of Narrow Gap Cadmium based Compounds (emis datareviews series n°10, 1994) pp. 64-71.

[15] Tregildas J.H., Polgreen T.L. and Chen M.C., Dislocations and electrical characteristics of HgCdTe, *J. Cryst. Growth* **86** (1988) 460-466.

[16] Ferré D.,Thesis, Lille (1987).

[17] Girault P., Barbot J.F. and Blanchard C., Electrical properties of n-Hg$_{0.8}$Cd$_{0.2}$Te plastically deformed, *J. Mat. Sci. Lett.* **14** (1995) 449-451.

[18] Barbot J.F., Kronewitz J. and Schröter W., Creation of p-n Junction in Hg$_{0.3}$Cd$_{0.7}$Te, *J. Appl. Phys. Lett.* **57** (1990) 2689-2691.

[19] Gelsdorf F. and Schröter W., DLTS study of the influence of plastic deformation on deep levels in n-type CdTe, *Phil. Mag. A* **4** (1984) L35.

[20] Wartlick B.O., Barbot J.F., Schröter W. and Blanchard C., Electromigration in Se-doped Hg$_{0.3}$Cd$_{0.7}$Te crystals, *Phys. Stat. Sol (a)* **148** (1995) 111-121.

[21] Zozime A., Hanke I. and Schröter W., Point defect interaction with α and β dislocation in InP, *Phys. Stat. Sol (a)* **138** (1993) 445-450.